

**Citation for published version:**

Ivarez-Vázquez, M. Á, Álvarez-Iglesias, P., De Uña-Álvarez, E., Quintana, B., Caetano, M., & Prego, R. (2020). Industrial supply of trace elements during the "Anthropocene": A record in estuarine sediments from the ria of ferrol (NW iberian peninsula). *Marine Chemistry*, 223, 103825. [doi:10.1016/j.marchem.2020.103825](https://doi.org/10.1016/j.marchem.2020.103825)

**Accepted Manuscript**

Link to published version: <https://doi.org/10.1016/j.marchem.2020.103825>

**General rights:**

© 2020 Elsevier B.V. This article is distributed under the terms and conditions of the Creative Commons Attribution-Noncommercial-NoDerivatives (CC BY-NC-ND) licenses <https://creativecommons.org/licenses/by-nc-nd/4.0/>

1 **Industrial supply of trace elements during the “Anthropocene”: a record in estuarine**  
2 **sediments from the Ria of Ferrol (NW Iberian Peninsula)**

3

4 Authors: Miguel Ángel Álvarez-Vázquez<sup>a,b,\*</sup>; Paula Álvarez-Iglesias<sup>c</sup>; Elena De Uña-Álvarez<sup>a</sup>;  
5 Begoña Quintana<sup>d</sup>; Miguel Caetano<sup>e</sup>; Ricardo Prego<sup>b</sup>

6

7 <sup>a</sup>Grupo GEAT, Depto. de Historia, Arte y Geografía, Area de Geografía Física (University of  
8 Vigo), 32004 Ourense, Spain

9 <sup>b</sup>Instituto de Investigaciones Marinas (IIM-CSIC), 36208 Vigo, Spain

10 <sup>c</sup>Servicio de Seguridad Alimentaria y Desarrollo Sostenible (CACTI-University of Vigo), 36310  
11 Vigo, Spain

12 <sup>d</sup>Laboratorio de Radiaciones Ionizantes, Departamento de Física Fundamental (University of  
13 Salamanca), 37007-Salamanca, Spain.

14 <sup>e</sup>Instituto Português do Mar e da Atmosfera (IPMA), 1449-006 Lisboa, Portugal

15

16 \* Corresponding autor (mianalva@uvigo.es)

17

18 **Abstract**

19

20 This work addresses the study of a sediment core retrieved in the estuary of the Grande-de-  
21 Xubia River (Ria of Ferrol), which is among the first industrialized areas in the Iberian Peninsula  
22 and has links to the shipbuilding industry since 1750. The chemical analysis of trace elements  
23 (i.e. As, Cd, Co, Cr, Cu, Hg, Mo, Ni, Pb, V, and Zn) was coupled with <sup>210</sup>Pb dating. The results span  
24 a period of about 130 years and cover the whole of the 20<sup>th</sup> century. Trace element  
25 anthropogenic fluxes accumulating in the sediments were calculated and show that human  
26 inputs are the most important sources for Cu, Cd, Hg and Zn, being, on average, well over the

27 natural loads. The temporal variation in the anthropogenic contaminants allows the  
28 identification of four main phases describing the human-natural input interactions, which in  
29 chronological order, are: (i) early industrialization, (ii) industrial acceleration or first industrial  
30 transition, (iii) industrial collapse, and (iv) an industrial maturity or a second industrial transition.

31

32 **Keywords:** chemostratigraphy, Industrial Revolution, risk elements, Pb-210 dating

33

### 34 **Highlights**

35

36 - Trace element anthropogenic fluxes were calculated.

37 - Copper, Cd, Hg and Zn are indicators of the historical human pressure in the area.

38 - True industrialization in the study area begins around 1945.

39 - The Great Acceleration in the industrial record was detected as between 1945 and 1973.

40

### 41 **1. Introduction**

42

43 Since humans entered the global industrial stage, “human activities have also grown to become  
44 significant geological forces” (Crutzen, 2002). The classification of a new chronostratigraphic  
45 epoch named “Anthropocene” is currently under evaluation by the International Commission  
46 on Stratigraphy (Zalasiewicz et al., 2017). Regardless of its formal definition (or not), the term is  
47 now widely used, being a cultural “zeitgeist” (Malhi, 2017) as a framework for a time marked by  
48 an exponential population growth, important alterations in natural dynamics, and an  
49 unprecedented quantity of anthropogenic materials entering the environment (Gaillardet et al.,  
50 2003; Lewis and Maslim, 2015). One of the most suitable environmental indicators highlighting  
51 human-nature interactions are sediments: they hold a memory of the current global alteration  
52 of geochemical cycles. Some trace elements such as Pb or Hg are recognized as

53 chemostratigraphic markers with enough distinctiveness to leave reliable signals in sediments  
54 (Zalasiewicz et al., 2011). Their study promotes the necessity of high resolution temporal signals  
55 such as annual accumulation rates of geochemical indicators, coupled with the use of  
56 radiometric dating techniques such as those based on  $^{210}\text{Pb}$ - $^{226}\text{Ra}$  with an accuracy of years to  
57 decades (Waters et al., 2018).

58

59 Trace elements, hereinafter TEs, are defined as any element presenting an average  
60 concentration below 100 parts per million atoms, or under  $100\text{ mg kg}^{-1}$  (IUPAC, 2014), in a given  
61 matrix. Some of them (i.e. Cu, Ni, Pb, Zn) are intimately linked to human activities, being  
62 common contaminants and elements of concern, and regarded as potentially toxic elements  
63 (Thornton et al., 2001) due to their possible harm to human health or ecosystem functioning.  
64 Rivers and coastal areas host many human activities such that estuaries are nowadays often the  
65 most impacted systems on the Earth (Brich et al., 2015) due to their being the ultimate end-  
66 point of anthropogenic waste materials, particularly during the industrial era. In this way, the  
67 Ria of Ferrol is linked to the beginnings of the Industrial Revolution in Spain through the  
68 development of the shipbuilding industry (Ocampo Suárez-Valdés and Ruiz García, 2017) and its  
69 establishment in 1750 as one of the most important naval headquarters in Spain, together with  
70 Cádiz and Cartagena. Two long cores previously retrieved from the middle part of the ria  
71 (Cobelo-García and Prego, 2003), showed a noticeable metal enrichment, mainly by Cu, Pb and  
72 Zn deposited during the industrial era. Other works on surficial sediments pointed to a higher  
73 impact in the middle part of this ria due to urban settlements and industrial activities (Cobelo-  
74 García et al., 2005), favored by a “restricted water exchange between the ria and the shelf”  
75 (Cobelo-García and Prego, 2004a). Nevertheless, the estuarine area was barely addressed.

76

77 The work herein presents the analysis and interpretation of the anthropogenic TEs inputs to the  
78 estuary of the Grande-de-Xubia River, developed in the head of the Ria of Ferrol. Using TEs as

79 indicators of human pressure, the aim is to characterize the human and natural processes  
80 interacting during the industrial era through the quantification of their anthropogenic fluxes  
81 recorded in estuarine sedimentary sequences.

82

## 83 **2. Study area**

84

85 Rias are particular coastal features, they are former fluvial valleys flooded by the sea after the  
86 last glacial maximum due to sea level rise. Their geomorphology is the result of glacioeustatic  
87 dynamics, tectonic structure and fluvial processes (Vidal Romaní, 1984; Méndez and Rey, 2000).

88 Rias were first described in a scientific context by the geographer Ferdinand Von Richthofen in  
89 1886 (Méndez and Vilas, 2005). A defining feature is that a ria has at least one small inner estuary

90 which can move in response to climatic changes (Evans and Prego, 2003). The Artabro Gulf (NW  
91 Iberian Peninsula, see Fig. 1) is featured by the confluence of four rias (i.e. Ferrol, Ares, Betanzos

92 and Coruña; sometimes a 5<sup>th</sup> ria is also included, that of Cedeira, located northward), formed by  
93 fluvial incision (incised valleys) during the Neogene (Vidal Romaní, 2018). Between them, the Ria

94 of Ferrol is a 15 km long valley covering a surface of 21 km<sup>2</sup> and containing about 0.25 km<sup>3</sup> of  
95 water (deCastro et al., 2004). The main continental watercourse is the Grande-de-Xubia River

96 (or Xubia River), which drains into the innermost part of the ria featuring a small estuary. This  
97 river has a watershed of 182 km<sup>2</sup> and an average flow of 5.77 m<sup>3</sup> s<sup>-1</sup> (Augas de Galicia, 2019).

98 The lithology of the basin is composed of schist with paragneiss, siltstones, amphibolites and  
99 graywackes, and alkaline and calcoalkaline granites (DHGC, 2016). It also contains two points

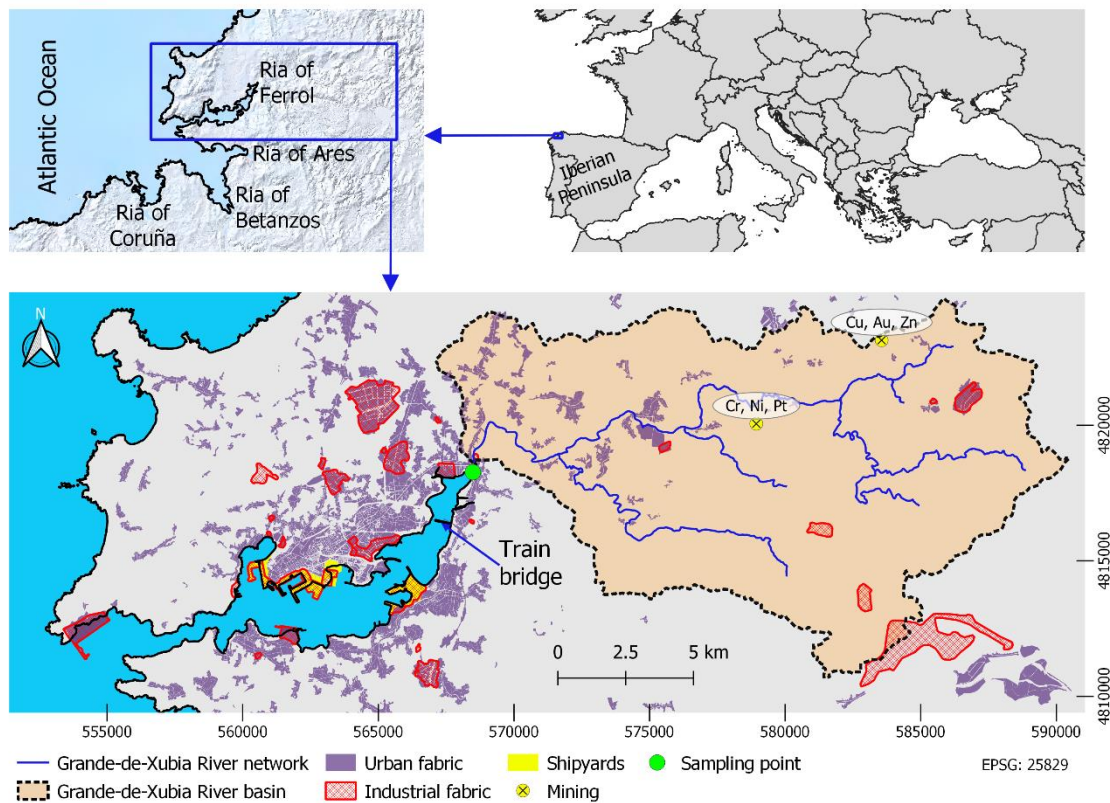
100 identified as mineral deposits (i.e. one with mineral associations of Cu, Fe, Au and Zn; and  
101 another with Fe, Cr, Ni and Pt; IGME, 2019; see location in Fig. 1). Land uses are highly modified,

102 a 41 % of the basin is dedicated to eucalyptus plantations, and a 35 % corresponds to cultivation  
103 fields, while around 9 % are artificial surfaces (IET, 2015). Population density is low in this basin,

104 about 163 inhab km<sup>-2</sup>, being more concentrated on the ria shore with an estimated 612 inhab

105 km<sup>2</sup> (data for year 2012, INEbase, 2019). It is important to note that, while the anthropogenic  
 106 enrichment of TEs in estuarine sediments seems to be historically related to population growth  
 107 in the Rias of Ares, Betanzos and Coruña (Álvarez-Vázquez et al., 2019), in the estuary of the  
 108 Xubia River (Cobelo-García and Prego, 2004b) the data point to pure industrial wastes as the  
 109 major contamination source of TEs.

110



112 Figure 1. Location map showing the sampling point together with selected human factors around  
 113 the Ria of Ferrol and the watershed of the Grande-de-Xubia River. Data from the Spanish  
 114 National Geographic Institute (© IGN) and Instituto de Estudos do Território da Consellería de  
 115 Medio Ambiente, Territorio e Infraestruturas (© Xunta de Galicia).

116

### 117 3. Material and Methods

118

119 A sediment short-core was hand collected in July 2012 in the estuary of the Xubia River (the  
120 innermost part of the Ria of Ferrol), in the intertidal muddy flats (43.5140N; 8.1528W), during  
121 low tide. A stainless steel hand-driven Gouge Augers Sampler, 61 mm inner-diameter and 70 cm  
122 long, was used. A 50 cm sediment column was recovered. The core was on-site sliced into 2 cm  
123 layers and stored in plastic zip-bags at 4° C. Once in the laboratory, core subsamples were dried  
124 at 45±5° C until constant weight. Dry sediment samples were grinded in an agate ball-mill to fine  
125 powders. Samples were split into three parts in order to perform different analyses, i.e. the  
126 organic matter content, the elemental contents, and dating by means of <sup>210</sup>Pb.

127

### 128 3.1. Chemical analysis

129

130 The contents of particulate organic carbon (POC) and sulphur (S) were determined by the  
131 Analytical Services of the University of A Coruña (SAI-UDC, Spain) using routine procedures.  
132 Sediments for POC determination were acid digested with HCl at 80° C to remove carbonates;  
133 then, POC was measured in an EA1108 Elemental Analyser (Carlo Erba Instruments). The S  
134 determination was performed on bulk samples in a FlashEA1112 Elemental Analyser  
135 (ThermoFinnigan). Replicates of a High Organic Sediment Standard (Elemental Microanalysis)  
136 was used to determine the precision of the methods, with the standard deviation lower than ±  
137 0.05% (n=6).

138

139 The contents of major elements (i.e. Al, Fe and Mn) were determined by Atomic Absorption  
140 Spectrometry in the Marine Biogeochemistry laboratory of the Marine Research Institute (IIM-  
141 CSIC, Spain). Previously, samples were digested (microwave-assisted) using a 3:1 mix of HNO<sub>3</sub>  
142 and HF in Teflon bombs following the US-EPA guideline 3052 (US-EPA, 1996). The final  
143 determination was conducted in a Flame Atomic Absorption Spectrometer (SpectrAA 220 FS,  
144 Varian inc.) with a nitrous oxide-acetylene flame (Al), or an air-acetylene flame (Fe and Mn). The

145 analysis of the content of trace elements (TEs; i.e. As, Cd, Co, Cr, Cu, Mo, Ni, Pb, V and Zn) was  
 146 carried out in the Environmental Oceanography laboratory of the Portuguese Institute of Sea  
 147 and Atmosphere (IPMA, Portugal). Samples were acid digested with HF and *Aqua Regia*  
 148 according to Rantala and Loring (1975). After that, TEs contents were determined in a  
 149 quadrupole ICP-MS (Thermo-Elemental X-series, Peltier impact bead spray chamber and  
 150 concentric Meinhard nebulizer) following the method described by Caetano et al. (2009). Total  
 151 mercury was also analysed in the IPMA by direct injection of the sample in an Atomic Absorption  
 152 Spectrometer (silicon UV diode detector Leco AMA-254); samples, in an oxygen-rich  
 153 atmosphere, were brought under pyrolysis (750° C) and Hg was collected on an Au-amalgamator  
 154 (Costley et al., 2000). The validity of the methods was checked by the analysis of the certified  
 155 sediment reference material PACS-2 (National Research Council of Canada). Results, which are  
 156 presented in Table 1, were in good agreement with the certified contents. Procedural blanks  
 157 were below the 1% of the element content of the samples.

158

**Table 1.** Control of the analytical procedure for the content determination of major and trace elements. Comparison between the analysed and the certified contents (n=5) for the certified reference material PACS-2 (NRC-Canada). Units are expressed in mg kg<sup>-1</sup> except for Al and Fe which are in g kg<sup>-1</sup>.

	Al	As	Cd	Co	Cr	Cu	Fe
Analysed	65.1±4.4	25.9±2.6	2.16±0.24	10.9±1.4	87.0±4.8	313±3	41.4±1.5
Certified	66.2±3.2	26.2±1.5	2.11±0.15	11.5±0.3	90.7±4.6	310±12	40.9±0.6
	Hg	Mn	Mo	Ni	Pb	V	Zn
Analysed	3.06±0.05	426±9	5.30±0.19	40.0±1.7	180±10	136±1	375±13
Certified	3.04±0.20	440±19	5.43±0.28	39.5±2.3	183±8	133±5	364±23

159

160



161 3.2. Core dating

162

163 Radionuclide analyses were performed in the Ionizing Radiation Laboratory (University of  
164 Salamanca, Spain), with a core resolution of 4 cm, in a Canberra n-type coaxial low-level  
165 background hyper-pure Germanium (HPGe) detector. The specific activities of  $^{210}\text{Pb}$ ,  $^{226}\text{Ra}$ ,  $^{214}\text{Pb}$   
166 and  $^{137}\text{Cs}$  were simultaneously determined. For details on source preparation, spiking, for  
167 equipment background and spectra analyses see Álvarez-Iglesias et al. (2007). All sediment  
168 radionuclide concentrations are given in  $\text{Bq}\cdot\text{kg}^{-1}$  dry weight. The  $^{210}\text{Pb}_{\text{xs}}$  specific activity was  
169 calculated by subtracting that for the  $^{214}\text{Pb}$  at 351.93 keV to that of the  $^{210}\text{Pb}$  (46.54 keV) for each  
170 sample, assuming secular equilibrium between  $^{226}\text{Ra}$  and the  $^{210}\text{Pb}_{\text{sup}}$  fraction (Pfitzner et al.,  
171 2004; San Miguel et al., 2004; Álvarez-Iglesias et al., 2007). The core temporal framework was  
172 determined by applying the CRS model (Constant Rate of Supply), but first the core missing  
173 inventory was obtained (Goldberg, 1963; Appleby and Oldfield, 1978, 1992; Appleby, 1998;  
174 Cochran et al., 1998; Sanchez-Cabeza and Ruiz-Fernández, 2012).

175

176 Once the chronology is established, the  $^{210}\text{Pb}$ -derived sedimentation rate can be estimated by  
177 dividing the length of each *i-th* interval by the time span resulting from the  $^{210}\text{Pb}$  chronology.

178

179 3.3. Reference values and anthropogenic inputs

180

181 TEs background levels (BL) can be estimated by the use of pristine references in similar  
182 physiographical areas (Birch, 2017). In this case the normalized (TE/Al ratios) background levels  
183 previously established for the nearby estuary of the Eume River (Ria of Ares,  $\text{NBL}_{\text{A}}$ ; Álvarez-  
184 Vázquez et al., 2017) were considered due to the similarity of the catchment lithology and similar  
185 geographic complexities (Fig 1). Thus, the TE/Al background ratios (NBLs) considered were:  $\text{As/Al}$   
186  $= 0.21\cdot 10^{-3}$ ,  $\text{Cd/Al} = 2.09\cdot 10^{-6}$ ,  $\text{Co/Al} = 0.15\cdot 10^{-3}$ ,  $\text{Cr/Al} = 1.05\cdot 10^{-3}$ ,  $\text{Cu/Al} = 0.32\cdot 10^{-3}$ ,  $\text{Hg/Al} =$

187  $1.09 \cdot 10^{-6}$ , Ni/Al =  $0.30 \cdot 10^{-3}$ , Pb/Al =  $0.36 \cdot 10^{-3}$ , V/Al =  $0.64 \cdot 10^{-3}$ , and Zn/Al =  $1.40 \cdot 10^{-3}$ . In the case  
188 of Mo, although a BL was not established for the Ria of Ares, the average Mo/Al ratio calculated  
189 by Álvarez-Vázquez et al. (2017) for sediments of  $24 \cdot 10^{-6}$  was considered in order to obtain a  
190 rough estimation. Although it can be made a direct comparison between the TEs contents  
191 ( $[TE_{tot}]_i$ ) and their corresponding BL (by calculating the Contamination Factor-CF, Eq. 1;  
192 Hakanson, 1980), it is better to consider the relationship between the content of a target  
193 element normalized with respect to the content of a conservative element in the sample in front  
194 of the corresponding NBL (that is, calculating the Enrichment Factor-EF, Eq. 2, Zoller et al., 1974).  
195 In this case Al was chosen as the normalizer element, as a good proxy to minimize the grain-size  
196 effect, as recommended for the Galician Rias (Rubio et al., 2000; Álvarez-Iglesias and Rubio,  
197 2012). This approach has been successfully applied in estuarine cores of nearby areas and  
198 elsewhere (e.g. Birch, 2017; Álvarez-Vázquez et al., 2017). The mathematical expressions of the  
199 indicated indexes are presented in the following equations:

200

201

$$\text{Eq. 1: } CF = [TE_{tot}]_i / BL$$

202

203

$$\text{Eq. 2: } EF = ([TE_{tot}]_i / [Al]_i) / NBL_A$$

204

205 The degree of contamination can be discussed according to the obtained CF and EF values. Then,  
206 the contamination criteria adopted were:  $EF \leq 1$  negligible,  $1 < EF \leq 3$  possible/moderate,  $3 < EF$   
207  $\leq 6$  considerable/severe,  $6 < EF \leq 9$  very severe and,  $EF > 9$  heavy (adapted from Hakanson, 1980;  
208 Prego et al., 2008).

209

210 Accordingly, The anthropogenic metal content ( $[TE_{anthr}]_i$ ), for each core subsample (*i*-th depth  
211 interval) and TE, can be estimated by subtracting the expected background TE content from the  
212 measured total TE content ( $[TE_{tot}]_i$ ). This expected background content was calculated

213 considering Al concentrations as a grain-size proxy (that is, based on TE/Al ratios; Álvarez-Iglesias  
214 et al., 2012):  $([Al]_i \cdot NBL_A)$ . This calculation was performed according to Eq. 3:

215

216 Eq. 3:  $[TE_{anthr}]_i = [TE_{tot}]_i - ([Al]_i \cdot NBL_A)$

217

218 Taking into account the established sedimentation rates, the TE fluxes to the sediment can also  
219 be calculated according to Eq. 4 (Cochran et al., 1998):

220

221 Eq. 4:  $F_i = s_i \cdot \rho_i \cdot [TE]_i$

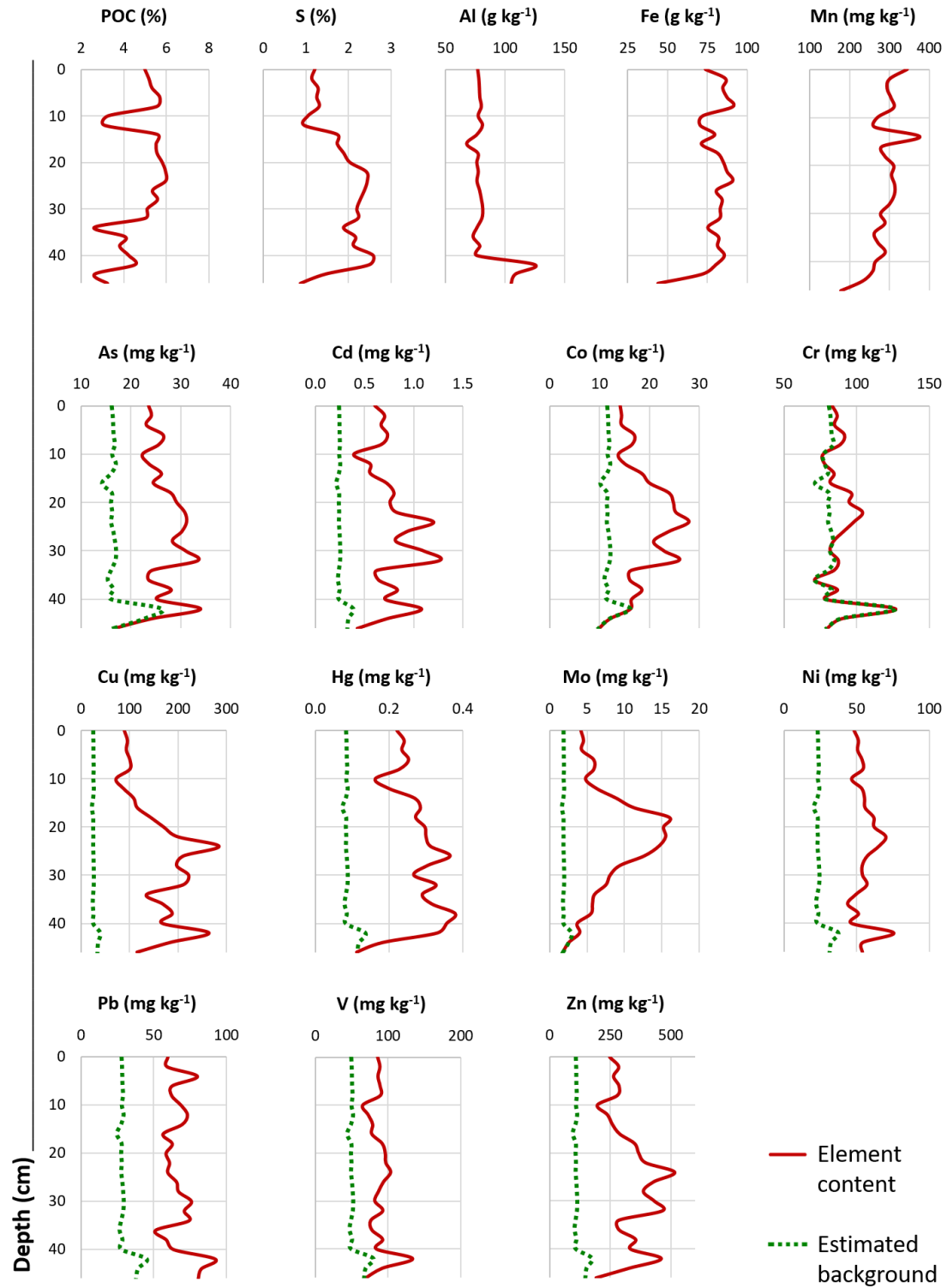
222

223 where  $F_i$  is the anthropogenic TE flux for the  $i$ -th depth interval ( $\text{mg cm}^{-2} \text{ yr}^{-1}$ );  $s_i$  is the  $^{210}\text{Pb}$ -  
224 derived sedimentation rate for the  $i$ -th interval ( $\text{cm yr}^{-1}$ );  $\rho_i$  is the dry bulk density ( $\text{g cm}^{-3}$ ) of the  
225  $i$ -th interval; and  $[TE]$  is the TE content for the  $i$ -th interval ( $\text{mg g}^{-1}$ ). Depending on the TE content  
226 considered (total:  $[TE_{tot}]$  or anthropogenic:  $[TE_{anthr}]$ ), the total and the anthropogenic fluxes can  
227 be respectively calculated.

228

229 **4. Results and discussion**

230



231

232 Figure 2. Depth profiles of key variables and trace elements in the core from the Ria of Ferrol.

233 The background estimation according to the Al content of each trace element is also presented

234 as a dotted line.

235

236 *4.1. Evaluation of general core contents of trace elements*

237

238 The summary statistics determined for the core contents of key variables (i.e. POC, S, Al, Fe and  
239 Mn) and trace elements (i.e. As, Cd, Co, Cr, Cu, Hg, Mo, Ni, Pb, V and Zn) are presented in Table  
240 2. On a consideration of the TE content profiles (Fig. 2), preindustrial deposits were not present  
241 in the core as expected considering that the area has been under shipbuilding pressure since  
242 1750. In order to perform a quick review-assessment, first, TEs contents in the studied sediments  
243 were compared to previously well-established local BLs: (i) one BL set determined in  
244 preindustrial layers from two long cores (1.6-1.8 m long) retrieved in the middle reach of the Ria  
245 of Ferrol in 1998 (Cobelo-García and Prego, 2003); (ii) another BL set determined in layers not  
246 affected by human activities (in this case those deposited before 1961) from a short core (0.5 m  
247 long) retrieved in the intertidal muddy flats of the Eume River Estuary, in the innermost part of  
248 the Ria of Ares (Álvarez-Vázquez et al., 2017), see Fig. 1. Both sets of BLs were compared and  
249 discussed by the aforementioned authors considering regional (e.g. Galician estuaries,  
250 Carballeira et al., 2000) and global scales (e.g. uncontaminated marine sediments, Doherty et  
251 al., 2000; composition of the upper continental crust, Rudnick and Gao, 2003).

252

253 In the data presented in Table 2, the TEs contents show, in general, well over the BL. Average CF  
254 values (Eq. 1) were 7-14 for Cu, 3-6 for Zn, 4 for Cd and Mo, 3 for Hg and Pb, 2-3 for Co and Ni  
255 and 2 for As and V. The lowest CF values were obtained for Cr (1.1). According to the considered  
256 contamination criteria there is a general heavy contamination by Cu; high for Zn, Cd and Hg;  
257 from moderate to high for Co and Ni; moderate for As and V; and from negligible to moderate  
258 for Cr. The Mo contents in the studied sediments are higher than those previously established  
259 for the Ria of Ares, and are also probably affected by diagenetic processes. If these Mo values  
260 are considered as BL, the Mo contents in the Ria of Ferrol would be indicative of a high  
261 contamination. Taking into account grain size variability for evaluating contamination, the EFs

262 (Eq. 2) for each element, arranged in decreasing order, were: 5.9±2.2 for Cu, 3.1±0.9 for Cd,  
 263 3.1±0.9 for Hg, 2.9±0.8 for Zn, 2.3±0.3 for Ni, 2.3±0.2 for Pb, 1.7±0.2 for V, 1.6±0.3 for As, 1.6±0.5  
 264 for Co and 1.0±0.1 for Cr. The average EF value for Mo was 4.1±2.4. In light of these results,  
 265 there is detected, on average, a considerable/severe contamination for Cu, Cd, Hg and probably  
 266 Mo, and a possible/moderate contamination for Zn, Ni, Pb, V, As and Co, while a possible Cr  
 267 contamination is negligible.

268

**Table 2.** Summary statistics of the elemental contents of the studied core. Average ( $\bar{x}$ ) and dispersion as standard deviation (SD) values, and the robust statistics of the 5-number summary (minimum, Min; quartile 1, Q1; median; quartile 2, Q2; and maximum, Max) are also presented. References for comparison are provided: baseline contents for the Ria of Ares (ARE, Álvarez-Vázquez et al., 2017) and background values for the Ria of Ferrol (FER, Cobelo-García and Prego, 2003).

	$\bar{x} \pm SD$	Min	Q1	median	Q3	Max	ARE	FER	
POC	48±11	26	41	52	56	60	21		%
S	18±5	9	13	19	22	26	4		
Al	83±14	68	77	79	81	125	75		g kg <sup>-1</sup>
Fe	77±17	11	74	82	85	91	62	24±5	"
Mn	284±40	177	265	289	305	377	326		mg kg <sup>-1</sup>
As	27±4	17	24	26	30	34	15		"
Cd	0.81±0.30	0.39	0.64	0.73	0.83	1.82	0.23		"
Co	19±5	10	15	17	24	28	11	6.1±1.5	"
Cr	88±11	71	82	87	92	127	78	63±14	"
Cu	165±77	72	101	167	199	410	24	12±3	"
Hg	0.27±0.07	0.11	0.23	0.27	0.31	0.38	0.09		"
Mo	7.6±4.2	1.8	4.5	6.0	9.4	16.0	1.9*		"

Ni	56±9	44	51	54	58	79	22	26±10	“
Pb	71±22	51	60	66	74	167	27	27±7	“
V	89±14	65	79	89	93	134	47		“
Zn	338±96	191	278	327	395	551	103	55±11	“

---

\* Rough estimation due to post-depositional mobilisation of Mo.

269

270 All these elements are common contaminants linked to the shipbuilding industry, according to  
 271 OECD (2010), with source in (i) base materials (i.e. Cd, Cr, Cu, Pb, Ni and Zn), (ii) surface coatings  
 272 (i.e. Cu, Cd, Cr, Pb and Zn), and (iii) abrasive blasting materials (i.e. As, Cd, Cr, Co, Pb, Ni and V);  
 273 but also linked to urban effluents (i.e. Cd, Cr, Cu, Hg, Ni, Pb and Zn; ICON, 2001). These results  
 274 agree with previous studies on subsurface middle ria sediments and on surficial sediments from  
 275 the Ria of Ferrol where contamination by Cd, Cu, Pb and Zn has been described (Cobelo-García  
 276 et al., 2005; Cobelo-García and Prego, 2003). In these studies maximum enrichments were  
 277 detected near contamination point-sources, and attributed to the discharge of untreated urban  
 278 and industrial wastewater, and magnified by accumulation of contaminants in this ria due to its  
 279 morphology (Cobelo-García and Prego, 2004a).

280

281 The natural and anthropogenic inputs to the study area were estimated for each sediment layer  
 282 (Eq. 3). The average natural inputs for each element are as follows: 17±2 mgAs kg<sup>-1</sup>, 0.25±0.04  
 283 mgCd kg<sup>-1</sup>, 12±1 mgCo kg<sup>-1</sup>, 83±10 mgCr kg<sup>-1</sup>, 26±4 mgCu kg<sup>-1</sup>, 0.089±0.014 mgHg kg<sup>-1</sup>, 25±4 mgNi  
 284 kg<sup>-1</sup>, 30±5 mgPb kg<sup>-1</sup>, 53±8 mgV kg<sup>-1</sup>, and 115±18 mgZn kg<sup>-1</sup>. A rough estimation for Mo is below  
 285 1.9±0.3 mg kg<sup>-1</sup>. The average anthropogenic contribution of TEs to the sediments, in decreasing  
 286 order, can be estimated as: 81±7 % for Cu, 65±13 % for Cd, 63±17 % for Hg, 63±12 % for Zn, 57±6  
 287 % for Pb, 55±6 % for Ni, 39±10 % for V, 34±12 % for As, 32±18 % for Co, and 5±7 % for Cr.

288

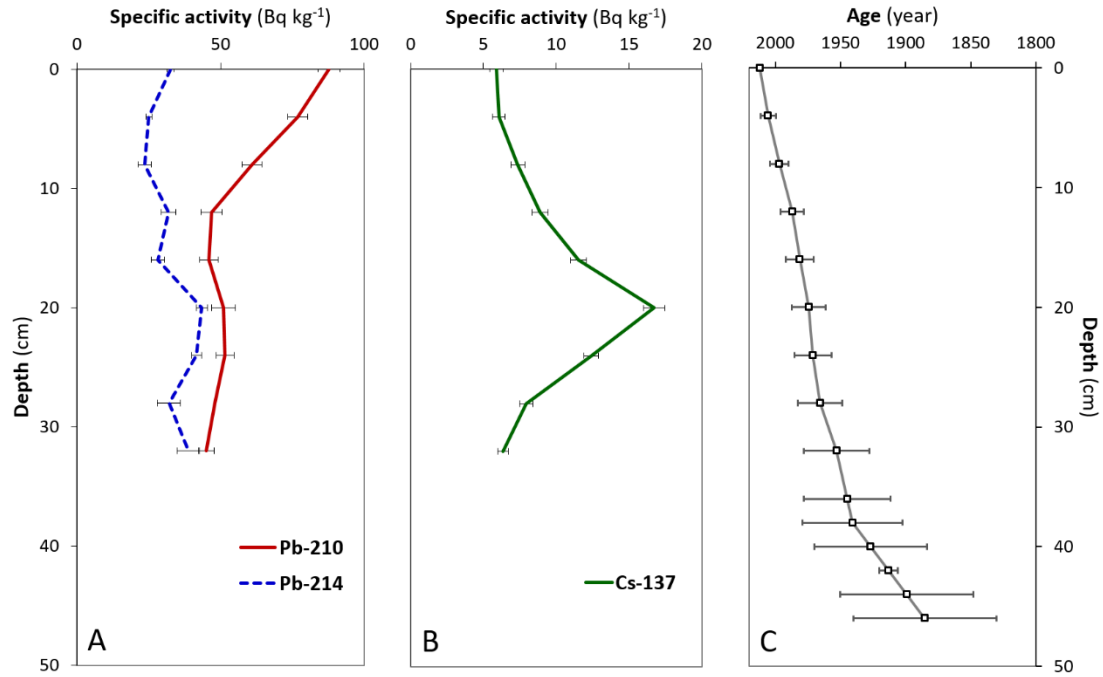
289 *4.2. Core chronology*

290

291 Specific activity profiles of  $^{214}\text{Pb}$ , total  $^{210}\text{Pb}$ , and  $^{137}\text{Cs}$  are shown in Fig. 3. The  $^{214}\text{Pb}$  specific  
292 activity was around  $32 \text{ Bq kg}^{-1}$ . Total  $^{210}\text{Pb}$  specific activity was highest at the surface, reaching  
293 values of  $87.8 \text{ Bq kg}^{-1}$ , and then, decreasing down the core until values about  $44.9 \text{ Bq kg}^{-1}$  at 36  
294 cm. The specific activity of  $^{210}\text{Pb}_{\text{xs}}$  decreased almost monotonically with depth, with maximum  
295 surface values of about  $55.3 \text{ Bq kg}^{-1}$ .  $^{210}\text{Pb}_{\text{xs}}$  was almost undetectable ( $6.2 \pm 4.9 \text{ Bq kg}^{-1}$ ) at 36 cm.  
296 The total  $^{210}\text{Pb}_{\text{xs}}$  inventory (considering an estimation of the missing inventory below 38 cm) was  
297  $4.65(53) \text{ kBq m}^{-2}$  and the corresponding  $^{210}\text{Pb}_{\text{xs}}$  flux was  $209(24) \text{ kBq m}^{-2}\cdot\text{yr}^{-1}$ . The  $^{137}\text{Cs}$  isotope  
298 was detected along the entire core. The specific activity of  $^{137}\text{Cs}$  was over  $4 \text{ Bq kg}^{-1}$ , and showed  
299 a maximum at 20-24 cm ( $16.7 \pm 0.7 \text{ Bq kg}^{-1}$ ). According to the  $^{210}\text{Pb}$  geochronology, this  
300 maximum corresponds to the year  $1974 \pm 7$ . Furthermore, in the  $^{137}\text{Cs}$  profile, peaks  
301 corresponding to the maximum inputs into the environment (1963, 1987; Nielsen, 1995;  
302 Andersen et al., 2000) were not observed for this radionuclide due to diagenetic mobilization  
303 (Davies et al., 1984; Zwolsman et al., 1993; Kim et al., 1997; Foster et al., 2006; Álvarez-Iglesias  
304 et al., 2007). Taking into account that  $^{210}\text{Pb}$  mobility is negligible under anoxic and moderately  
305 sulfidic conditions (Crusius and Anderson, 1991), the obtained  $^{210}\text{Pb}$  chronology is reliable, but  
306 needs to be validated by other techniques independent of age control. In this case,  
307 anthropogenically induced changes in the environment have been considered, as discussed  
308 below. The chronological framework based in  $^{210}\text{Pb}$  CRS dating covers the last  $67 \pm 33$  years (36  
309 cm depth). The estimated average sediment accumulation rate for this dated period was around  
310  $6.2 \text{ mm yr}^{-1}$ . The gradual reduction in the obtained  $^{210}\text{Pb}_{\text{xs}}$  activity depth-profile points to a  
311 progressive accumulation, without remobilisation of sediments, at least since the year  $1945 \pm 33$ .

312





313

314 Figure 3. Depth profiles of  $^{210}\text{Pb}$ - $^{214}\text{Pb}$  (A),  $^{137}\text{Cs}$  (B) and the results of the depth/age model (C)  
 315 in the core from the estuary of the Grande-de-Xubia River, Ria of Ferrol.

316

317 In the depth-profiles of As, Cd, Co, Zn and Cu (Fig. 2), a change from lower to higher  
 318 anthropogenic TE contents can be observed (i.e. considering the difference between the  
 319 estimated background and the measured total content), that, according to the  $^{210}\text{Pb}$  chronology,  
 320 would have occurred between  $1953 \pm 25$  (32 cm) and  $1971 \pm 14$  (24 cm). This change is also  
 321 observed in the POC profile. The maximum anthropogenic input is clear in the profiles of Cu and  
 322 Zn at 24 cm depth, and could be related to the rupture of a mining settlement pond situated  
 323 inside the Xubia River basin, which happened in the early 1960s, and thus, corroborates the  $^{210}\text{Pb}$   
 324 chronology. The mine exploited massive Cu-sulphide deposits which presented mineral  
 325 associations of Fe, Au and Zn (IGME, 2019). The incident, as described in the testimonies,  
 326 involved a significant release of contaminated sludge into the river, and therefore, into the  
 327 estuary. In addition, diagenetic processes can modify TEs profiles leading to certain element  
 328 peaks (Álvarez-Iglesias and Rubio, 2008; Huerta-Díaz and Morse, 1990), such as those observed  
 329 at 24 cm in the studied core.

330

331 Aluminium content is relatively constant from the surface to 40 cm depth ( $77.7 \pm 2.9 \text{ g kg}^{-1}$ ),  
332 increasing by less than 145 % on average ( $113 \pm 11 \text{ g kg}^{-1}$ ; Fig. 2). This element is commonly used  
333 as a lithogenic proxy due to its presence as a major constituent of rocks and its relationship with  
334 clay minerals (Birch, 2017). This change is also clearly marked in the depth-profiles of other  
335 elements, such as Ni and Cr, elements that are mainly bound to silicates in intertidal and subtidal  
336 ria sediments (Álvarez-Iglesias and Rubio, 2008, 2009). Thus, the marked change in Al contents  
337 at 40-42 cm could be pointing to a change in the hydrodynamics of the system. This could result  
338 from the construction of a railway bridge in 1913 (Yáñez, 2008) with a breakwater that covers  
339 around three quarters of the bridge length, and which affected the water circulation patterns in  
340 the area, and allowed the settling of fine-grained sediments. According to the  $^{210}\text{Pb}$  model,  
341 sediments below 40 cm deposited before  $1945 \pm 33$ , and thus, around the year of the bridge  
342 construction, were assigned to the sample located at 42 cm. Taking into account this temporal  
343 marker, sedimentation rates around  $1.4 \text{ mm yr}^{-1}$  were obtained for the bottom samples of the  
344 core. When extrapolating this rate downwards, the studied core will correspond to an estimated  
345 period of about 130 years (until 46 cm). Sedimentation rates were low until 1966 ( $< 5 \text{ mm yr}^{-1}$ ),  
346 and then rose markedly until 1974 (exceeding  $12 \text{ mm yr}^{-1}$ ), then decreased until 1997 (around  $4$   
347  $\text{mm}\cdot\text{yr}^{-1}$ ), and finally slightly increased up to 2012 ( $> 6 \text{ mm yr}^{-1}$ ). According to the established  
348 temporal framework, the estimated  $^{210}\text{Pb}_{\text{xs}}$  fluxes are about  $200 \text{ Bq}\cdot\text{m}^{-2}\cdot\text{yr}^{-1}$ , coherent with the  
349 expected atmospheric fluxes (around  $120\text{-}140 \text{ Bq m}^{-2} \text{ yr}^{-1}$ ; Appleby, 1998) for the study area,  
350 considering mean annual rainfall (around  $1000\text{-}1200 \text{ mm}$ ; Castillo Rodríguez et al., 2006).

351

352 *4.3. Integrated view*

353

354 From a consideration of the time-variation of the anthropogenic fluxes of TEs to the sediments  
 355 (calculated according Eq. 3) and the Enrichment Factors (EFs, Eq.2), four phases are  
 356 distinguishable (Table 3 and Fig. 4):

357

Table 3. Anthropogenic fluxes of trace elements to the sedimentary record of the Grande-de-Xubia Estuary (Ria of Ferrol). Results are divided into four stages of industrial development in the area and presented as mg m<sup>-2</sup> yr<sup>-1</sup>- minimum (median) maximum.

	<b>Early Ind.</b>	<b>Acceleration</b>	<b>Collapse</b>	<b>Maturity</b>
	Before 1945	1945-1975	1975-2000	After 2000
As	nd (8.3) 10.9	18 (49) 80	14 (28) 42	12 (18) 21
Cd	0.15 (0.49) 0.79	0.9 (3.0) 3.2	0.4 (1.3) 1.5	0.7 (0.9) 1.3
Co	nd (2.3) 6.3	14 (47) 78	5 (20) 33	4.9 (6.2) 11.0
Cr	nd - 3.6	nd (25) 125	nd (12) 40	3.8 (8.2) 18.5
Cu	119 (149) 253	269 (687) 968	118 (257) 355	127 (145) 195
Hg	nd (0.23) 0.28	0.3 (0.7) 1.2	0.20 (0.47) 0.78	0.27 (0.32) 0.43
Ni	22 (28) 43	47 (117) 261	48 (104) 138	50 (58) 77
Pb	25 (44) 62	60 (146) 184	53 (100) 178	63 (80) 96
V	3 (32) 61	56 (149) 275	41 (91) 127	67 (78) 108
Zn	64 (222) 323	430 (1180) 1594	227 (522) 652	275 (329) 482

*Ind.: Industrialization; nd: non detected*

358

359 (i) **Early industrialization:** before 1945. The year 1750 is considered to be the beginning of this  
 360 period because, at this time, the ria had become a strategic centre of military shipbuilding and  
 361 Navy settlement, and it was also coupled with both a strong auxiliary industry (González-Llanos  
 362 Galvache, 1996; Franco Castañón, 2008) and the exploitation of mineral deposits within the river  
 363 basin (Castroviejo Bolibar et al., 2004). This period was identified in two long cores retrieved in

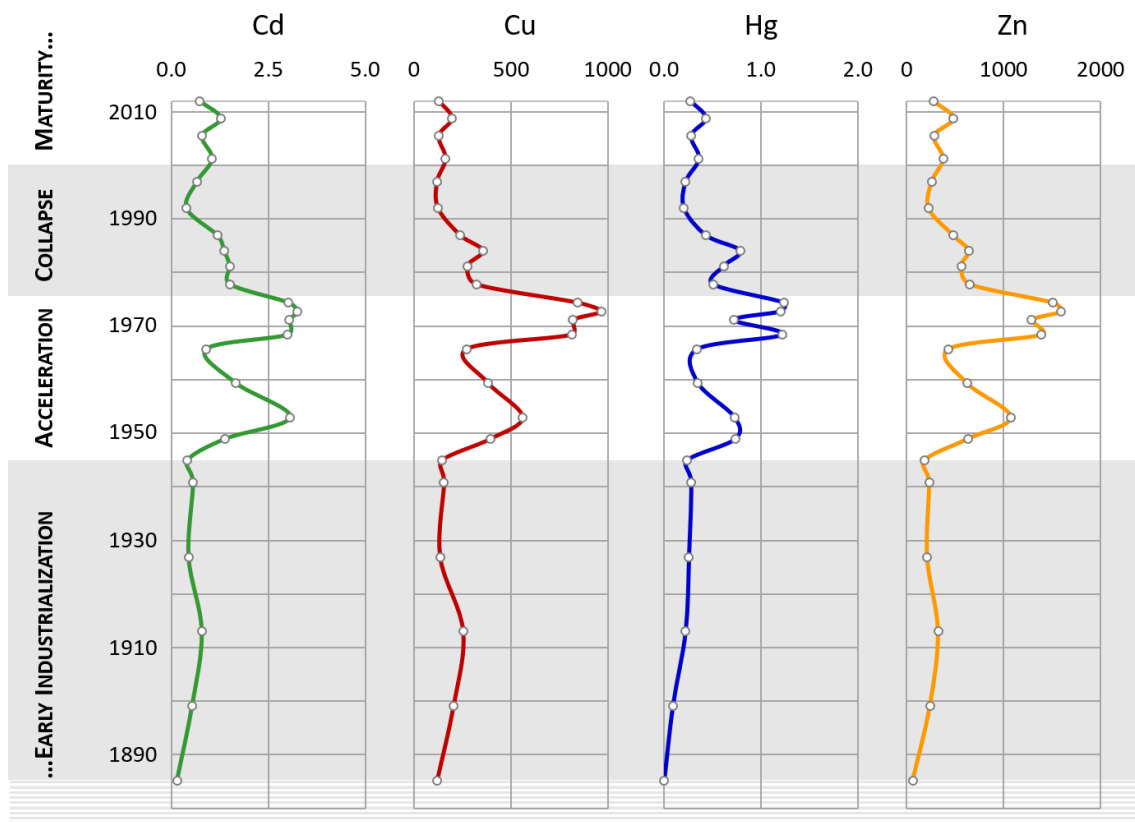
364 the centre of the middle ria by Cobelo-García and Prego (2003) by a marked upwards enrichment  
365 in the TEs contents depth-profiles. In the studied estuarine sediments, this stage is depicted by  
366 the enrichments of Cu and Cd, and, to a lesser extent, Hg, Zn and Pb. Average EFs in this lowest  
367 part of the core were indicative of a very severe contamination by Cu (EF = 6.1),  
368 considerable/severe by Cd (EF = 3.8), and possible/moderate for Hg (EF = 2.9), Zn (EF = 2.5) and  
369 Pb (EF = 2.1). The average anthropogenic sediment fluxes can be arranged by relative  
370 importance, as the anthropogenic average and percentage of the total TE flux, as follows: Cu  
371 ( $168 \text{ mg m}^{-2} \text{ yr}^{-1}$ , 82%) > Cd ( $0.48 \text{ mg m}^{-2} \text{ yr}^{-1}$ , 57%) = Zn ( $205 \text{ mg m}^{-2} \text{ yr}^{-1}$ , 57%) > Pb ( $44 \text{ mg m}^{-2}$   
372  $\text{yr}^{-1}$ , 52%) > Hg ( $0.18 \text{ mg m}^{-2} \text{ yr}^{-1}$ , 54%) > Ni ( $29 \text{ mg m}^{-2} \text{ yr}^{-1}$ , 48%) > V ( $33 \text{ mg m}^{-2} \text{ yr}^{-1}$ , 33%) > As  
373 ( $6.3 \text{ mg m}^{-2} \text{ yr}^{-1}$ , 23%) > Co ( $2.7 \text{ mg m}^{-2} \text{ yr}^{-1}$ , 16%) > Cr ( $0.60 \text{ mg m}^{-2} \text{ yr}^{-1}$ , 1%). As can be seen in  
374 Fig. 4, the trend between 1885 and 1945 is relatively constant or with a slight tendency to  
375 increase.

376

377 (ii) **Industrial acceleration or first industrial transition:** 1945 - 1973. The true industrialization  
378 observed after 1945 is in agreement with the work of Álvarez-Vázquez et al. (2017). These  
379 authors frame the generalization of industrialization in the area after the Spanish Civil War  
380 (1936-1939). With the support of the dictatorship, Ferrol developed an important modern  
381 industry for military shipbuilding but also, aimed to produce civil vessels. Between the 1930s  
382 and the 1950s the industry underwent modernization and restructuring to be competitive in an  
383 international context. Production experienced a great expansion, particularly after 1962,  
384 employing more than 20,000 people (Cardesín, 2004). In this period, and related to the  
385 exploitation of mineral deposits within the river basin (sulphides with mineral associations of  
386 Cu, Au and Zn; Fig. 1), the previously mentioned breakage of a Cu-mine pond in the early 1960s  
387 could introduce into the estuary important amounts of TEs (the authors did not find any citable  
388 reference for this event, nor the precise date; it is only supported by oral unauthenticated oral  
389 statements). There is also an important source of contamination in this period (Prego et al.,

390 2003), a siderurgy arose in 1939 to recycle iron and steel by-products from the shipyards, and it  
391 located on the shore of the estuary. In between 1945 and 1975, almost all the studied TEs  
392 increase their contamination indexes, particularly Cu (average EF in this period = 8.1, with a peak  
393 of 11.6 in 1971) and Cd (EF = 5.7, with a peak of 7.5 in 1971); also Zn (EF = 3.7), Hg (EF = 3.6), Ni  
394 (EF = 2.5), Pb (EF = 2.4) and Co (EF = 2.0). In decreasing order, the average importance in TEs  
395 fluxes was observed to be as follows: Cu ( $632 \text{ mg m}^{-2} \text{ yr}^{-1}$ , 87%), Cd ( $2.4 \text{ mg m}^{-2} \text{ yr}^{-1}$ , 73 %), Zn  
396 ( $1066 \text{ mg m}^{-2} \text{ yr}^{-1}$ , 72 %), Hg ( $0.82 \text{ mg m}^{-2} \text{ yr}^{-1}$ , 72 %), Ni ( $134 \text{ mg m}^{-2} \text{ yr}^{-1}$ , 60 %), Pb ( $134 \text{ mg m}^{-2}$   
397  $\text{yr}^{-1}$ , 57 %), Co ( $44 \text{ mg m}^{-2} \text{ yr}^{-1}$ , 49 %), V ( $155 \text{ mg m}^{-2} \text{ yr}^{-1}$ , 44 %), As ( $48 \text{ mg m}^{-2} \text{ yr}^{-1}$ , 44 %), and Cr  
398 ( $40 \text{ mg m}^{-2} \text{ yr}^{-1}$ , 9 %). All the TEs present similar profiles (see selected elements in Fig. 4). An  
399 accelerated increase was detected, with maxima in the late 1960s-early 1970s, as observed e.g.  
400 in the Bay of Cadiz in the second half of the 20<sup>th</sup> century (Ligero et al., 2002 ) as consequence of  
401 industrial and urban impacts. For example, the increase in the Cu fluxes to the sediment can be  
402 adjusted to a straight line with a slope of  $19.5 \text{ mg m}^{-2} \text{ yr}^{-1}$  ( $r = 0.70$ ,  $n = 8$ ). This phase is  
403 simultaneous with the so-called “Great Acceleration” that happened in the mid-20<sup>th</sup> century  
404 (Steffen et al., 2007; 2011), delineated, together with other indicators, by an important release  
405 of TEs (Pb and other metals) into the environment as result of industrialization (Lewis and  
406 Maslim, 2015).

407



408

409 Figure 4. Temporal evolution of the anthropogenic TEs fluxes to the sediment in the estuary of  
 410 the Grande-de-Xubia River (Ria of Ferrol) and identification of four different phases. Results are  
 411 presented in  $\text{mg m}^{-2} \text{yr}^{-1}$ .

412

413 (iii) **Industrial collapse:** 1973 – 2000. At this stage, the effects of the 1970s international  
 414 recession are similar to the collapse of economic growth following the Second World War  
 415 (Tausig and Fenwick, 1999). In the particular case of Ferrol, together with the international crisis  
 416 according to Cardesín (2004) there are several possibly responsible factors such as the socio-  
 417 economic instability in the 1970s, just before the change of the political regime; and also the  
 418 internationalization of Spain in the 1980s, with its entry in the European Economic Community.  
 419 These resulted in policies of naval reconfiguration that highly impacted the shipyards of the ria.  
 420 Additionally, some information places the closure of Cu-mine in the late 1960s, but closure of  
 421 mining activities is not usually followed by a drastic decrease in sediment contamination, e.g. as  
 422 observed in the sedimentary registry of the Nalón Estuary and the Asturias' coast, N. Spain

423 (García-Ordiales et al. 2020 ; García-Ordiales et al. 2017 ). During this period of recession, the  
424 EFs drastically decay. Only Cu and Cd present average EFs around 4 (4.3 and 3.9, respectively),  
425 the Cu levels drops to a possible/moderate contamination. The average fluxes to the sediment  
426 at this stage are: Cu ( $239 \text{ mg m}^{-2} \text{ yr}^{-1}$ , 75 %), Hg ( $0.46 \text{ mg m}^{-2} \text{ yr}^{-1}$ , 62 %), Cd ( $1.1 \text{ mg m}^{-2} \text{ yr}^{-1}$ , 59  
427 %), Zn ( $470 \text{ mg m}^{-2} \text{ yr}^{-1}$ , 58 %), Pb ( $116 \text{ mg m}^{-2} \text{ yr}^{-1}$ , 58 %), Ni ( $95 \text{ mg m}^{-2} \text{ yr}^{-1}$ , 58 %), V ( $88 \text{ mg m}^{-2}$   
428  $\text{yr}^{-1}$ , 37 %), As ( $26 \text{ mg m}^{-2} \text{ yr}^{-1}$ , 35 %), Co ( $19 \text{ mg m}^{-2} \text{ yr}^{-1}$ , 33 %), and Cr ( $16 \text{ mg m}^{-2} \text{ yr}^{-1}$ , 6 %). The  
429 trend in the last quarter of the 20<sup>th</sup> century reflects an important reduction in the anthropogenic  
430 inputs. Again the example of Cu is illustrative, adjusting to a straight line the slope is  $-12.3 \text{ mg}$   
431  $\text{m}^{-2} \text{ yr}^{-1}$  ( $r = 0.88$ ,  $n = 6$ ).

432

433 (iv) **Industrial maturity or second industrial transition**, after 2000. With the new millennium the  
434 naval industry in Ferrol was reactivated thanks to new policy strategies (Cardesín, 2004). This  
435 increase in the industrial activity is not accompanied by an increase in the anthropogenic  
436 contributions of TEs to the estuary. The adoption of environmental protection regulations  
437 coming from the European Union lead to better production systems and a reduction in human  
438 pressure on the ecosystems. This effect was also observed in the industrialized Ria of Bilbao  
439 (Fdez-Ortiz de Vallejuelo, 2010), or even in low industrialized areas related to the  
440 implementation of the urban wastewater treatment after the European Water Framework  
441 Directive (Álvarez-Vázquez et al., 2018). For the first time, Cd is the element that shows the  
442 highest average EF (4.1) followed by Cu (3.8), both remaining at levels of possible/moderate  
443 contamination. Mercury (2.8), Zn (2.5), Pb (2.3) and Ni (2.2) present average EFs slightly higher  
444 than 2. These enrichments are not necessarily linked to new anthropogenic inputs, as observed  
445 by Cobelo-García and Prego (2004b), because the resuspension of contaminated sediments in  
446 the estuary can be acting as secondary contamination source. During this stage, sediments fluxes  
447 are estimated as follows: Cu ( $153 \text{ mg m}^{-2} \text{ yr}^{-1}$ , 74 %), Cd ( $1.0 \text{ mg m}^{-2} \text{ yr}^{-1}$ , 64 %), Hg ( $0.33 \text{ mg m}^{-2}$   
448  $\text{yr}^{-1}$ , 64 %), Zn ( $354 \text{ mg m}^{-2} \text{ yr}^{-1}$ , 59 %), Pb ( $80 \text{ mg m}^{-2} \text{ yr}^{-1}$ , 56 %), Ni ( $61 \text{ mg m}^{-2} \text{ yr}^{-1}$ , 54 %), As (17

449 mg m<sup>-2</sup> yr<sup>-1</sup>, 32 %), Co (7.1 mg m<sup>-2</sup> yr<sup>-1</sup>, 21 %) and Cr (9.6 mg m<sup>-2</sup> yr<sup>-1</sup>, 5 %). The TEs content profiles  
450 during this stage remain relatively constant (Fig. 4).

451

452 These phases are coherent with the environmental zones previously described in the  
453 sedimentary record of the Bilbao estuary by Cearreta et al. (2002) attributed to the impact of  
454 untreated domestic and industrial effluents. These zones are: pre-industrial (not achieved in  
455 Ferrol), older industrial (early industrialization) and younger industrial (acceleration). The work  
456 herein describes two additional phases in the sequence: collapse and maturity. The first and  
457 second industrial transitions were denominated due to the similarity and chronological  
458 parallelism with the population dynamics described for the theories of the First and Second  
459 Demographic Transitions (e.g. van de Kaa, 2002).

460

## 461 **5. Concluding remarks**

462

463 The estuary of the Grande-de-Xubia River has been surrounded by important industrial activities  
464 since the middle of the 18<sup>th</sup> century. Its sediments are a suitable record to study the impact and  
465 evolution of anthropogenic inputs during the industrial era. The studied core covers 130 years,  
466 since 1885, reflecting an acceleration in the human inputs after 1945, when it can be stated that  
467 the true industrial era had started. Copper, Cd, Zn and Hg are the most illustrative contaminants,  
468 reaching maximum signals around the early 1970s, presenting enrichment factors up to 11.6,  
469 7.5, 4.8 and 4.2, respectively. The average amounts of anthropogenic trace elements entering  
470 in the sedimentary record were 82 % for Cu, 64 % for Cd and Hg, 63 % for Zn. Four phases were  
471 distinguished by: (i) an early industrialization denoted by a relatively low impact; followed by (ii)  
472 an acceleration between 1945 and 1973, that could be related to the mid-20<sup>th</sup> century “Great  
473 Acceleration”, presenting the highest values for contamination indexes; (iii) a collapse in the  
474 industrial activity, denoting the effects of the 1970s global crisis, which means a drastic fall of



475 anthropogenic contributions to the sedimentary record; and (iv) an industrial reactivation after  
476 2000, when more environmental friendly processes responding to protection policies result in a  
477 low contamination.

478

479 **Acknowledgments:** This study was financed by the project “Land-sea exchange of trace metals  
480 and its importance for marine phytoplankton in an upwelling coast”, ref. CTM2011-28792-C02  
481 financed by the Spanish Ministry of Economy and Competitiveness. We thank our project fellows  
482 for their kind cooperation, especially to his coordinator Dr. Manuel Varela, recently deceased  
483 (Prego et al., 2020); also to María Lema Grille (SAI-UDC) for C and S elemental analyses. Dr.  
484 Jonathan Bould is warmly acknowledged for proofreading the final version of the manuscript.  
485 M.A. Álvarez-Vázquez is supported by the Xunta de Galicia through the postdoctoral grant  
486 #ED481B-2019-066.

487

#### 488 REFERENCES

- 489 Álvarez-Iglesias, P., Quintana, B., Rubio, B., Pérez-Arlucea, M., 2007. Sedimentation rates and  
490 trace metal input history in intertidal sediments derived from  $^{210}\text{Pb}$  and  $^{137}\text{Cs}$  chronology.  
491 J. Environ. Radioact. 98, 229-250.
- 492 Álvarez-Iglesias, P., & Rubio, B., 2012. Trace metals in shallow marine sediments from the Ría de  
493 Vigo: sources, pollution, speciation and early diagenesis. Earth's System Processes.  
494 INTECH Open Access Publisher, 185-210.
- 495 Álvarez-Iglesias, P., Rubio, B., Millos, J., 2012. Isotopic identification of natural vs. anthropogenic  
496 lead sources in marine sediments from the inner Ría de Vigo (NW Spain). Sci. Total  
497 Environ. 437, 22-35.
- 498 Álvarez-Iglesias, P., Rubio, B., 2008. The degree of trace metal pyritization in subtidal sediments  
499 of a mariculture área: Application to the assessment of toxic risk. Mar. Pollut. Bull. 56,  
500 973-983.

501 Álvarez-Iglesias, P., Rubio, B., 2009. Redox status and heavy metal risk in intertidal sediments in  
502 NW Spain as inferred from the degrees of pyritization of iron and trace elements. *Mar.*  
503 *Pollut. Bull.* 58, 542-551.

504 Álvarez-Vázquez, M.A., De Uña-Álvarez, E., Prego, R., 2019. 20th century urban changes in the  
505 land-to-ocean fluvial transport of trace metals. In Álvarez-Vázquez, M.A. & De Uña-  
506 Álvarez, E. (Coords.) *Perspectivas del Agua. Investigación, gestión y valores del agua en el*  
507 *mundo actual.* Dykinson, pp 67-83.

508 Álvarez-Vázquez, M.A., González-Prieto, S.J., Prego, R., 2018. Possible impact of environmental  
509 policies in the recovery of a Ramsar wetland from trace metal contamination. *Sci. Total*  
510 *Environ.* 637, 803-812.

511 Álvarez-Vázquez, M.A., Caetano, M., Álvarez-Iglesias, P., del Canto Pedrosa-García, M., Calvo, S.,  
512 De Uña-Álvarez, E., Quintana, B., Vale, C., Prego, R., 2017. Natural and Anthropocene  
513 fluxes of trace elements in estuarine sediments of Galician Rias. *Estuarine Coastal Shelf*  
514 *Sci.* 198, 329-342.

515 Andersen, T.J., Mikkelsen, O.A., Møller, A.I., Pejrup, M., 2000. Deposition and mixing depths on  
516 some European intertidal mudflats based on  $^{210}\text{Pb}$  and  $^{137}\text{Cs}$  activities. *Cont. Shelf Res.* 20,  
517 1569-1591.

518 Appleby, P.G., 1998. Dating recent sediments by  $^{210}\text{Pb}$ : problems and solutions. In: Ilus, E. (Ed.),  
519 *Dating of sediments and determination of sedimentation rate. Proceedings of a seminar*  
520 *held in Helsinki 2-3 April 1997.* STUK-A 145, Helsinki, pp. 7-24.

521 Appleby, P.G., Oldfield, F., 1978. The calculation of  $^{210}\text{Pb}$  dates assuming a constant rate of  
522 supply of unsupported  $^{210}\text{Pb}$  to the sediment. *Catena* 5, 1-8.

523 Appleby, P.G., Oldfield, F., 1992. Application of Lead-210 to sedimentation studies. In Ivanovich,  
524 M., Harmon, R.S. (Eds.), *Uranium-series Disequilibrium Applications to Earth, Marine and*  
525 *Environmental Sciences,* Clarendon Press, Oxford, pp. 731-778.

526 Augas de Galicia, 2019. Ficha de estación de aforo Nº 446 – Xubia.  
527 [https://augasdegalicia.xunta.gal/c/document\\_library/get\\_file?file\\_path=/portal-augas-](https://augasdegalicia.xunta.gal/c/document_library/get_file?file_path=/portal-augas-)  
528 [de-galicia/redeAforos/446-Xubia\\_es\\_gl.pdf](https://augasdegalicia.xunta.gal/c/document_library/get_file?file_path=/portal-augas-de-galicia/redeAforos/446-Xubia_es_gl.pdf) (last accessed 19.11.04).

529 Birch, G.F., 2017. Determination of sediment metal background concentrations and enrichment  
530 in marine environments—a critical review. *Sci. Total Environ.* 580, 813-831.

531 Birch, G.F., Gunns T.J., Olmos, M., 2015. Sediment-bound metals as indicators of anthropogenic  
532 change in estuarine environments. *Mar. Pollut. Bull.* 101, 243-257.

533 Caetano, M., Prego, R., Vale, C., dePablo, H., Marmolejo-Rodríguez, J., 2009. Evidence for early  
534 diagenesis of rare earth elements and metals in a transition sedimentary environment.  
535 *Mar. Chem.* 116, 36-46.

536 Cardesín, J.M. 2004. 'Historia de dos Ciudades'. La Memoria de Ferrol, entre la Marina de Guerra  
537 y la Clase Trabajadora. Cambridge Journals.  
538 [https://www.researchgate.net/profile/Jose\\_Cardesin\\_Diaz/publication/301216156\\_'Historia\\_de\\_dos\\_Ciudades'\\_La\\_Memoria\\_de\\_Ferrol\\_entre\\_la\\_Marina\\_de\\_Guerra\\_y\\_la\\_Clas\\_e\\_Trabajadora/links/570ce0a908ae2b772e42a176.pdf](https://www.researchgate.net/profile/Jose_Cardesin_Diaz/publication/301216156_'Historia_de_dos_Ciudades'_La_Memoria_de_Ferrol_entre_la_Marina_de_Guerra_y_la_Clas_e_Trabajadora/links/570ce0a908ae2b772e42a176.pdf) (last accessed 19.06.25)

541 Castillo Rodríguez, F., Martínez Cortizas, A., Blanco Chao, R., 2006. O clima de Galicia. In:  
542 Narango, L., Pérez Muñuzuri, V. (Coords.). A variabilidade natural do clima en Galicia.  
543 Consellería de Medio Ambiente e Desenvolvemento Sostible (Xunta de Galicia), pp. 19-  
544 91.

545 Carballeira, A., Carral, E., Puente, X., Villares, R., 2000. Regional-scale monitoring of coastal  
546 contamination. Nutrients and heavy metals in estuarine sediments and organisms on the  
547 coast of Galicia (northwest Spain). *Int. J. Environ. Pollut.* 13, 534-572.

548 Castroviejo Bolibar, R., Armstrong, E., Lago, A., Martínez Simón, J.M., Argüelles, A., 2004.  
549 Geología de las Mineralizaciones de Sulfuros Masivos en los cloritoesquistos de Moeche  
550 (Complejo de Cabo Ortegal, La Coruña). *Bol. Geol. Min.* 115(1), 3-34.

551 Cearreta, A., Irabien, M. J., Leorri, E., Yusta, I., Quintanilla, A., Zabaleta, A., 2002. Environmental  
552 transformation of the Bilbao estuary, N. Spain: microfaunal and geochemical proxies in  
553 the recent sedimentary record. *Mar. Pollut. Bull.* 44(6), 487-503.

554 Cobelo-García, A., Labandeira, A., Prego, R., 2005. Two opposite cases of metal accumulation in  
555 ria sediments: Ferrol and Corme-Laxe (Galicia, NW Iberian Peninsula). *Ciencias Marinas*  
556 31(4), 653-659.

557 Cobelo-García, A., Prego, R., 2004a. Influence of point sources on trace metal contamination and  
558 distribution in a semi-enclosed industrial embayment: the Ferrol Ria (NW Spain).  
559 *Estuarine Coastal Shelf Sci.* 60(4), 695-703.

560 Cobelo-Garcia, A., Prego, R., 2004b. Behaviour of dissolved Cd, Cu, Pb and Zn in the estuarine  
561 zone of the Ferrol ria (Galicia , NW Iberian Peninsula). *Fresen. Environ. Bull.* 13(8), 753-  
562 759.

563 Cobelo-García, A., Prego, R., 2003. Heavy metal sedimentary record in a Galician Ria (NW Spain):  
564 background values and recent contamination. *Mar. Pollut. Bull.* 46(10), 1253-1262.

565 Cochran, J.K., Frignani, M., Salamanca, M., Bellucci, L.G., Guerzoni, S., 1998. Lead-210 as a tracer  
566 of atmospheric input of heavy metals in the northern Venice Lagoon. *Mar. Chem.* 62, 15-  
567 29.

568 Costley, C.T., Mossop, K.F., Dean, J.R., Garden, L.M., Marshall, J., Carroll, J., 2000. Determination  
569 of mercury in environmental and biological samples using pyrolysis atomic absorption  
570 spectrometry with gold amalgamation. *Anal. Chim. Acta* 405, 179-183.

571 Crusius, J., Anderson, R.F., 1991. Imobility of <sup>210</sup>Pb in Black Sea sediments. *Geochim.*  
572 *Cosmochim. Acta* 55, 327-333.

573 Crutzen, P.J., 2006. The “Anthropocene”. In: *Earth System Science in the Anthropocene*.  
574 Springer, Berlin, Heidelberg, pp. 13-18.

575 Davies, R.B., Hess, C.T., Norton, S.A, Hanson, D.W., Hoagland, K.D., Anderson, D.S., 1984. <sup>137</sup>Cs  
576 and <sup>210</sup>Pb dating of sediments from soft-water lakes in New England (U.S.A) and  
577 Scandinavia, a failure of <sup>137</sup>Cs dating. Chem. Geol. 44, 151-185.

578 Doherty, G.B., Coomans, D., Brunskill, G.J., 2000. Modelling natural and enhanced trace metal  
579 concentrations in sediments of Cleveland Bay, Australia. Mar. Freshwater Res. 51, 739-  
580 747.

581 DeCastro, M., Gomez-Gesteira, M., Prego, R., Alvarez, I., 2004. Ria–ocean exchange driven by  
582 tides in the Ria of Ferrol (NW Spain). Estuarine Coastal Shelf Sci. 61(1), 15-24.

583 DHGC (2016) Plan Hidrológico da Demarcación Hidrográfica de Galicia-Costa 2015-2021,  
584 Capítulo 2. Descripción xeral da Demarcación. Demarcación Hidrográfica de Galicia-Costa,  
585 144pp. [https://augasdegalicia.xunta.gal/c/document\\_library/get\\_file?file\\_path=/portal-](https://augasdegalicia.xunta.gal/c/document_library/get_file?file_path=/portal-augas-de-galicia/plans/PHGC-2015-2021/Cap02_PGHC20152021_gl.pdf)  
586 [augas-de-galicia/plans/PHGC-2015-2021/Cap02\\_PGHC20152021\\_gl.pdf](https://augas-de-galicia/plans/PHGC-2015-2021/Cap02_PGHC20152021_gl.pdf) (last accessed  
587 17.11.20).

588 Doherty, G.B., Coomans, D., Brunskill, G.J., 2000. Modelling natural and enhanced trace metal  
589 concentrations in sediments of Cleveland Bay, Australia. Mar. Freshwater Res. 51, 739-  
590 747.

591 Evans, G., Prego, R., 2003. Rias, estuaries and incised valleys: is a ria an estuary?. Mar. Geol.  
592 196(3-4), 171-175.

593 Fdez-Ortiz de Vallejuelo, S., Arana, G., de Diego, A., Madariaga, J.M., 2010. Risk assessment of  
594 trace elements in sediments: the case of the estuary of the Nerbioi–Ibaizabal River  
595 (Basque Country). J. Hazard. Mater. 181(1):565-573.

596 Foster, I.D.L., Mighall, T.M., Proffitt, H., Walling, D.E., Owens, P.N., 2006. Post-despositional <sup>137</sup>Cs  
597 mobility in the sediments of three shallow coastal lagoons, SW England. J. Paleolimnol.  
598 35, 881-895.

599 Franco Castañón, H., 2008. La sociedad española de construcción naval, Cuaderno nº57 del  
600 Instituto de Historia y Cultura Naval, 39-49.

601 Gaillardet, J., Viers, J., Dupré, B., 2005. Trace Elements in River Waters. In: Holland, H.D.,  
602 Turekian, K.K. (Eds.), Treatise on Geochemistry. Vol. 5. Elsevier, pp. 225-272.

603 García-Ordiales, E., Flor-Blanco, G., Roqueñí, N., Covelli, S., Cienfuegos, P., Álvarez, R., Frontolan,  
604 G., Loredó, J., 2020. Anthropocene footprint in the Nalón estuarine sediments (northern  
605 Spain). *Mar. Geol.* 424, 106167.

606 García-Ordiales, E., Cienfuegos, P., Roqueñí, N., Covelli, S., Flor-Blanco, G., Fontolan, G., Loredó,  
607 J., 2019. Historical accumulation of potentially toxic trace elements resulting from mining  
608 activities in estuarine salt marshes sediments of the Asturias coastline (northern Spain).  
609 *Environ. Sci. Pollut. R.* 26(4), 3115-3128.

610 Goldberg, E.D., 1963. Geochronology with  $^{210}\text{Pb}$ . In: Radioactive dating, International Atomic  
611 Energy Agency, Vienna, pp. 121-131.

612 González-Llanos Galvache, S., 1996. La construcción naval en Ferrol durante el siglo XIX. In: Ferrol  
613 en la estrategia marítima del siglo XIX. XV Jornadas de Historia Marítima, Instituto de  
614 Historia y Cultura Naval, 19-52.

615 Hakanson, L., 1980. An ecological risk index for aquatic pollution control. A sedimentological  
616 approach. *Water Res.* 14(8), 975-1001.

617 Huerta-Díaz, M.A., Morse, J.W., 1990. A quantitative method for determination of trace metal  
618 concentrations in sedimentary pyrite. *Mar. Chem.* 29, 119-144.

619 ICON, 2001. Pollutants in urban waste water and sewage sludge. European Commission.  
620 Luxembourg.  
621 [https://ec.europa.eu/environment/archives/waste/sludge/pdf/sludge\\_pollutants.pdf](https://ec.europa.eu/environment/archives/waste/sludge/pdf/sludge_pollutants.pdf)  
622 (last accessed 19.10.21)

623 IET, 2015. Mapa de usos do solo, IDE Información Xeográfica de Galicia, Instituto de Estudos do  
624 Territorio, Xunta de Galicia, <http://mapas.xunta.gal/visores/basico/> (accessed 15.11.16).

625 IGME, 2019. Mapa de metalogenia (yacimientos e indicios minerales). Instituto Geológico y  
626 Minero de España. <http://info.igme.es/visorweb/> (last accessed 19.11.04).

627 INEbase, 2015. Cifras de población y Censos demográficos. Spanish Statistical Office.  
628 [http://www.ine.es/inebmenu/mnu\\_cifraspob.htm](http://www.ine.es/inebmenu/mnu_cifraspob.htm) (last accessed 19.11.04).

629 IUPAC, 2014. Compendium of Chemical Terminology – The Gold Book. International Union of  
630 Pure and Applied Chemistry. <https://goldbook.iupac.org/> (last accessed 17.04.04).

631 Kim, G., Hussain, N., Church, T.M., Carey, W.L., 1997. The fallout isotope  $^{207}\text{Bi}$  in a Delaware salt  
632 marsh: a comparison with  $^{210}\text{Pb}$  and  $^{137}\text{Cs}$  as a geochronological tool. *Sci. Total Environ.*  
633 196, 31-41.

634 Lewis, S.L., Maslin, M.A., 2015. Defining the Anthropocene. *Nature* 519(7542), 171-180.

635 Ligeró, R.A., Barrera, M., Casas-Ruiz, M., Sales, D., López-Aguayo, F., 2002. Dating of marine  
636 sediments and time evolution of heavy metal concentrations in the Bay of Cádiz, Spain.  
637 *Environ. Pollut.* 118(1), 97-108.

638 Luoma, S.N., Dagovitz, R., Axtmann, E., 1990. Temporally intensive study of trace metals in  
639 sediments and bivalves from a large river-estuarine system: Suisun Bay/Delta in San  
640 Francisco Bay. *Sci. Total Environ.* 97, 685-712.

641 Malhi, Y., 2017. The concept of the Anthropocene. *Annu. Rev. Environ. Resour.* 42, 77-104.

642 Méndez, G., Vilas, F., 2005. Geological antecedents of the Rias Baixas (Galicia, northwest Iberian  
643 Peninsula). *J. Mar. Syst.* 54(1-4), 195-207.

644 Méndez, G., Rey, D., 2000. Perspectiva histórica del conocimiento geológico de las rías gallegas.  
645 *J. Iber. Geol.* 26, 21-44.

646 Nielsen, S.P., 1995. A box model for North-East Atlantic coastal waters compared with  
647 radioactive tracers. *J. Mar. Syst.* 6, 545-560.

648 Ocampo Suárez-Valdés, J.C., 2018. Los arsenales del Rey: 1750-1820, la revolución industrial que  
649 pudo haber sido, Glyphos Publicaciones, Valladolid (Spain).

650 OECD, 2010. Environmental and climate change issues in the shipbuilding industry. OECD Council  
651 Working Party on Shipbuilding (WP6). <https://www.oecd.org/sti/ind/46370308.pdf>  
652 (accessed 19.08.26)

653 Pfitzner, J., Brunskill, G., Zgorskis, I., 2004.  $^{137}\text{Cs}$  and excess  $^{210}\text{Pb}$  deposition patterns in estuarine  
654 and marine sediment in the central region of the Great Barrier Reef Lagoon, North-Eastern  
655 Australia. *J. Environ. Radioact.* 76, 81-102.

656 Prego, R., Bode, A., Bao, R., 2020. Obituary. Manuel Varela Rodriguez. *Sci. Mar.* 84 (1): 103-104.

657 Prego, R., Ferro, P., Trujillo, C., 2008. Lead and Zinc contamination of surface sediments in the  
658 main harbours of the Galician Rias. *J. Iber. Geol.* 34 (2) 2008: 243-252

659 Prego, R., García, A. C., Tubío, C., del Carmen Barciela, M., 2003. Presence, distribution and  
660 contamination levels of lead in the surface sediments of the Ria of Ferrol (NW Spain).  
661 *Cienc. Mar.* 29(4), 561-571.

662 Rantala, R., Loring, D., 1975. Multi-element analysis of silicate rocks and marine sediments by  
663 atomic absorption spectrophotometry. *Atomic Absorption Newsletter* 14, 117-120.

664 Rubio, B., Nombela, M.A., Vilas, F., 2000. Geochemistry of Major and Trace Elements in  
665 Sediments of the Ria de Vigo (NW Spain): an Assessment of Metal Pollution. *Mar. Poll.*  
666 *Bull.* 40, 968-980.

667 Rudnick, R. L., Gao, S., 2003. Composition of the continental crust, in: *Treatise on Geochemistry*,  
668 3, 1-64.

669 Ruiz, F., 2001. Trace metals in estuarine sediments from the southwestern Spanish coast. *Mar.*  
670 *Poll. Bull.* 42, 481-489.

671 San-Miguel, E.G., Bolívar, J.P., García-Tenorio, R., 2004. Vertical distribution of Th-isotope ratios,  
672  $^{210}\text{Pb}$ ,  $^{226}\text{Ra}$  and  $^{137}\text{Cs}$  in sediment cores from an estuary affected by anthropogenic  
673 releases. *Sci. Total Environ.* 318, 143-157.

674 Sanchez-Cabeza, J.A., Ruiz-Fernández, A.C., 2012.  $^{210}\text{Pb}$  sediment radiochronology: An  
675 integrated formulation and classification of dating models. *Geochim. Cosmochim. Acta*  
676 82, 183-200.



677 Steffen, W., Grinevald, J., Crutzen, P., McNeill, J., 2011. The Anthropocene: conceptual and  
678 historical perspectives. *Philosophical Transactions of the Royal Society A: Mathematical,*  
679 *Physical and Engineering Sciences* 369(1938), 842-867.

680 Steffen, W., Crutzen, P.J., McNeill, J.R., 2007. The Anthropocene: are humans now overwhelming  
681 the great forces of nature. *AMBIO* 36(8), 614-622.

682 Tausig, M., Fenwick, R., 1999. Recession and well-being. *J. Health Soc. Behav.* 1-16.

683 Thornton, L., Butler, D., Docx, P., Hession, M., Makropoulos, C., McMullen, M., Nieuwenhuijsen,  
684 M., Pitman, A., Rautiu, R., Sawyer, R., Smith, S., White, D., Wilderer, P., Paris, S., Marani,  
685 D., Braguglia, C., Palerm, J., 2001. *Pollutants in Urban Waste Water and Sewage Sludge.*  
686 *Final report prepared by IC Consultants, London, for Directorate-General Environment,*  
687 *European Commission, Office for Official Publications of the European Communities,*  
688 *Luxembourg.*

689 US-EPA, 1996. Method 3052. Microwave Assisted Acid Digestion of Siliceous and Organically  
690 Based Matrices. <http://www.epa.gov/epaoswer/hazwaste/test/3052.pdf> (last accessed  
691 15.04.07).

692 Van de Kaa, D.J., 2002. The idea of a second demographic transition in industrialized countries.  
693 [http://websv.ipss.go.jp/webj-ad/WebJournal.files/population/2003\\_4/Kaa.pdf](http://websv.ipss.go.jp/webj-ad/WebJournal.files/population/2003_4/Kaa.pdf) (last  
694 accessed: 19.10.18)

695 Vidal Romaní, J.R., 2018. La historia geológica de la formación del Golfo Ártabro (Coruña), In:  
696 *Patrimonio Natural e Cultural do Golfo Ártabro, CEIDA, 6-15.*

697 Vidal Romaní, J.R., 1984. A orixe das Rías Galegas. Estado da cuestión (1886-1983). *Actas do*  
698 *Primeiro Seminario de Ciencias do Mar: As Rías Galegas. Publicacións do Seminario de*  
699 *Estudos Galegos, 13-25.*

700 Waters, C.N., Fairchild, I.J., McCarthy, F.M., Turney, C.S., Zalasiewicz, J., Williams, M., 2018. How  
701 to date natural archives of the Anthropocene. *Geol. Today* 34(5), 182-187.

702 Yáñez, A., 2008. *Historia de Neda, Ría de Ferrol y comarca, Concello de Neda.*

703 Zalasiewicz, J., Waters, C. N., Summerhayes, C. P., Wolfe, A. P., Barnosky, A. D., Cearreta, A.,  
704 Crutzen, P., Ellis, E., Fairchild, I. J., Gałuszka, A., Haff, P., Hajdas, I., Head, M. J., Ivar do Sul,  
705 J. A., Jeandel, C., Leinfelder, R., McNeill, J. R., Neal, C., Odada, E., Oreskes, N., Steffen, W.,  
706 Syvitski, J., Vidas, D., Wapreisch, M. Williams, M., 2017. The Working Group on the  
707 Anthropocene: Summary of evidence and interim recommendations. *Anthropocene* 19,  
708 55-60.

709 Zalasiewicz, J., Williams, M., Fortey, R., Smith, A., Barry, T. L., Coe, A. L., Bown, P. R., Rawson, P.  
710 F., Gale, A., Gibbard, P., Gregory, F. J., Hounslow, M. W., Kerr, A. C., Pearson, P., Knox, R.,  
711 Powell, J., Waters, C., Marshall, J., Oates, M. Stone, F., 2011. Stratigraphy of the  
712 Anthropocene. *Philos. Trans. R. Soc. London, Ser. A* 369(1938), 1036-1055.

713 Zoller, W.H., Gladney, E.S., Gordon, G.E., Bors, J.J., 1974. Emissions of trace elements from coal  
714 fired power plants. In: Hemphill, D.D. (Ed.), *Trace Substances in Environmental Health*.  
715 Rolla, University of Missouri, Columbia, 8, 167-172.

716 Zwolsman, J.J., Berger, G.W., Van Eck, G.T.M., 1993. Sediment accumulation rates, historical  
717 input, postdepositional mobility and retention of major elements and trace metals in salt  
718 marsh sediments of the Scheldt estuary, SW Netherlands. *Mar. Chem.* 44, 73-94.

719